Load Shed Recovery with Transmission Switching and Intentional Islanding Methods after (N-2) Line Contingencies

Hussain, Tanveer; Ishaq, Saima; Liaqat, Sheroze; Zia, Muhammad Fahad; Al-Durra, Ahmed; Khan, Baseem; Guerrero, Josep M.

Published in:
IEEE Access

DOI (link to publication from Publisher):
10.1109/ACCESS.2022.3206376

Publication date:
2022

Document Version
Publisher's PDF, also known as Version of record

IEEE Access
Multidisciplinary ⋮ Rapid Review ⋮ Open Access Journal

Received 26 August 2022, accepted 8 September 2022, date of publication 12 September 2022,
date of current version 22 September 2022.

Digital Object Identifier 10.1109/ACCESS.2022.3206376

RESEARCH ARTICLE

Load Shed Recovery With Transmission Switching and Intentional Islanding Methods After (N-2) Line Contingencies

TANVEER HUSSAIN[1], (Member, IEEE), SAIMA ISHAQ[2], (Graduate Student Member, IEEE), SHEROZE LIAQAT[2], MUHAMMAD FAHAD ZIA[3,4], (Member, IEEE), AHMED AL-DURRA[4], (Senior Member, IEEE), BASEEM KHAN[5], (Senior Member, IEEE), AND JOSEP M. GUERRERO[6], (Fellow, IEEE)

[1]Idaho National Laboratory (INL), Idaho Falls, ID 83402, USA
[2]Department of Electrical Engineering and Computer Science, South Dakota State University (SDSU), Brookings, SD 57007, USA
[3]Department of Electrical Engineering, National University of Computer and Emerging Sciences, Lahore 54000, Pakistan
[4]Advanced Power and Energy Center (APEC), Department of Electrical Engineering and Computer Science, Khalifa University, Abu Dhabi, United Arab Emirates
[5]Department of Electrical and Computer Engineering, Hawassa University, Hawassa 1530, Ethiopia
[6]Center for Research on Microgrids (CROM), Department of Energy Technology, Aalborg University, 9220 Aalborg, Denmark

Corresponding author: Baseem Khan (baseem.khan04@gmail.com)

ABSTRACT Changing power system configuration may result in load shed recovery (LSR) because topology change can provide power flow control in meshed network. Some topologies may favor generation redispatch as compared to others and can eliminate line congestion which leads to LSR. One of the known methods for topology change is called transmission switching (TS) and research conducted in the past showed that TS is an effective means of mitigating load shedding. However, another method of topology control also exits and it is referred as intentional islanding (IIS). In this manuscript, we explore IIS as a potential solution for LSR. IIS based on generator coherency has been presented in literature for mitigating cascading failures. However, IIS has not been explored solely as a LSR mechanism. In this paper, we compare the LSR based on IIS with well known LSR algorithm based on TS. The comparison is performed for IEEE 39-bus system and IEEE 118-bus system. The results show that IIS has a potential to perform better than TS in terms of computational efficiency and LSR.

INDEX TERMS Contingency analysis, load shed recovery, intentional islanding, transmission switching, topology control.

I. INTRODUCTION

Power systems, now a days, are being operated close to their stability limits due to increasing electricity demand. One of the main goals of power system operators is to keep the power system secure and stable while meeting the variable power demand. However, in case of a disturbance, for example line outage, the nearby lines have to carry the weight of the failed lines' power. This rerouting of power flows may cause overload of various lines, thus resulting in a cascade of failures. Cascading failures, which are a series of successive power failures that propagate throughout the power system, cause large socioeconomic damages. The 2003 North American blackout, for instance, was the result of two line outages in the state of Ohio that left about 55 million people without electricity. One such recent event was the blackout in South America in June 2019 which affected Argentina and parts of Brazil, Paraguay, and Uruguay [1]. In such instances, load shedding might be the only solution to prevent cascading failures and keep the system stable.

Researchers in the past have developed algorithms to minimize the amount of load shed while also preventing cascading failures [2]. Topology control has been proven useful for load shed recovery (LSR). Topology changes can provide power

The associate editor coordinating the review of this manuscript and approving it for publication was Nagesh Prabhu.

flow control in meshed networks because some topologies may favor generation redispatch as compared to other topologies [3], [4]. In this paper, we consider two types of topology control methods. One is named Transmission Switching (TS) [5], [6], and the other is known as intentional islanding (IIS) [7], [8]. The aim of this paper is to compare these two topology control methods with respect to computational efficiency and amount of load shed recovered after N-2 line contingencies. These two methods have been discussed in the past but no comparison amongst the two exists. In this paper, we try to fill this gap by comparing these methods in terms of LSR and computational efficiency. In the past, IIS has been discussed as a mitigation scheme for cascading failures. This work however, explores IIS as a LSR mechanism. LSR algorithms based on TS have been developed in [9] and [10]. In this manuscript, we compare IIS based LSR algorithm with a well known TS based LSR algorithm.

The novelty and main contribution of this work are the simulation-based demonstration of an IIS method that can perform better than existing TS algorithms with the following features: i) no MIP based modification to optimal power flow (OPF) formulation as done in [10] and [11]; ii) at least one order of magnitude faster than LSB_{max} algorithm when seeking a solution for the IEEE 39-bus and IEEE 118-bus system [12]; iii) better LSR than the CE/ESM, LBTS, and LSB_{max} algorithms [12], [13].

The rest of the paper is organized as follows. Section II introduces TS and IIS, respectively. Section III introduces the DC optimal power flow (DCOPF) and AC optimal power flow (ACOPF) based formulation used in TS and IIS algorithms. Section IV describes the experimental setup. Section V describes the results and comparison between the IIS and the CE/ESM algorithm. Subsection V-D compares the IIS algorithm with the existing computationally fast TS algorithms from literature. Section VI concludes the findings.

II. PRELIMINARIES

A. TRANSMISSION SWITCHING (TS)

TS is a planned line outage. Removing a line from the power system changes its topology and the new configuration may result in generation redispatch which can reduce load shedding. This concept was first introduced in 1980s. Research in the past has shown TS as an effective means of reducing line overloads [9], [14], reduction of line losses [9], corrective voltage violations [15], security enhancement [16], and improving economic dispatch [17], [18] using machine learning algorithms [19] and in hydro-electric context [20]. TS based-resiliency model is proposed for extreme weather event scenarios [21]. Stochastic optimal TS model is developed to improve the power system security margins under renewable uncertainties [22]. TS aware mixed-integer linear programming model is developed for multi-scenario transmission network expansion planning (TNEP) problem [23]. Moreover, TS is also used for LSR [24], [25], which is the main focus of this paper. Despite of all its advantages, TS is being used by industries on limited occasions [9], [26]. One of the main reasons for its limited use is the complex or computationally expensive algorithms proposed in literature to find the best TS candidate for larger systems [26].

Complete enumeration (CE), [9], or exhaustive search method (ESM) [10] is one of the well known methods to find the best TS candidate. This method involves switching lines, one by one, one at a time to find the best TS candidate. Fig. 1 shows a flowchart for CE/ESM. For understanding, consider CE/ESM as a two step process, where the first level (shaded green color) determines the list of unfaulted branches that needs to be checked. The blocks shown in shaded color (orange) represent the choice of either the ACOPF or DCOPF formulation. Note that the CE/ESM algorithm is agnostic to the choice of formulation. In the second step, the branches from the list will be tested to find the best TS candidate with minimum load shedding. Assuming that electrical power system is N-1 compliant, we consider non-trivial N-2 contingencies. Non-trivial contingencies are a subset of contingencies that require load shedding even after generation redispatch. Note that the proposed algorithm is valid for any N-k line contingencies, where k = 1,2,3,..n. After detecting a non-trivial contingency, the algorithm removes/switches a line to check whether load shedding is improved or not. This process is repeated for all healthy lines in the system. Switching a line that results in minimum amount of load shed is the best TS candidate. An advantage of CE/ESM is the guarantee of finding a TS candidate for LSR, thus making it the standard base case for comparing newer algorithms [9], [10]. CE/ESM performs well for small systems but for larger systems, with a multitude of lines, the process of switching each line and running DC optimal power flow (DCOPF) to find the best TS candidate is computationally expensive and potentially intractable in time.

In [11], a computationally less expensive mixed integer program heuristic algorithm (MIP-H) is presented. But, large-scale test of MIP-H algorithm showed that it is not scalable. Researchers in [10] presented a mixed-integer programming model for AC power flows (MIPAC). MIPAC is a modification of an existing mixed-integer linear optimization model called linear-programming approximation of AC power flows (LPAC) model [27]. LPAC is computationally slower than CE/ESM. When seeking the best single switching action for IEEE 118-bus system, replacing CE/ESM by MIPAC resulted in an average speedup of approximately 2.3 times.

In [13], researchers presented the limit branches TS (LBTS) algorithm, based on line flow thresholds, which performs approximately 108 times faster than the CE/ESM for the IEEE 118-bus system. Although LBTS is computationally fast, results showed that it is capable of recovering only 5.2% of load shed compared to CE/ESM after (*N-2*) line contingencies for the IEEE 118-bus system. In [12], authors proposed the LSB_{max} algorithm based on selecting the candidate for TS using proximity to the load shedding bus where the most load is expected to be shed after a contingency. The LSB_{max} algorithm performs approximately 22 times faster than the

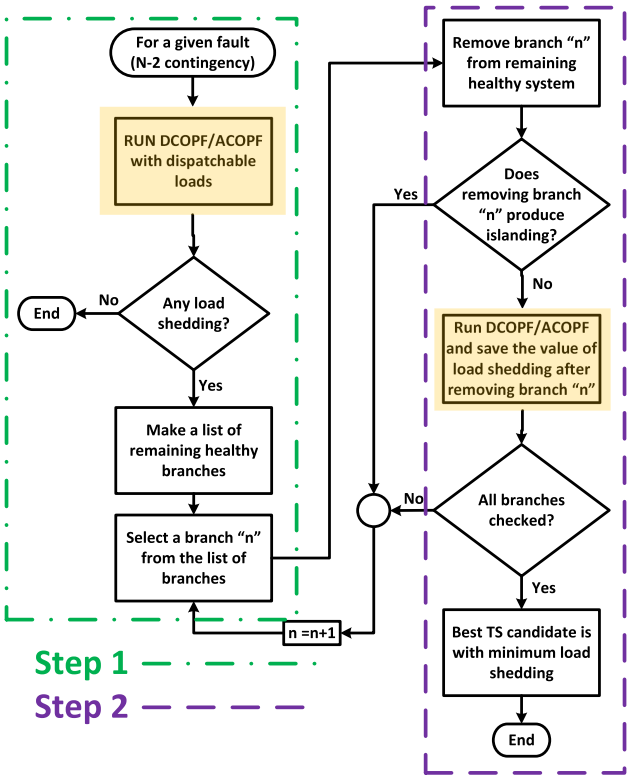

FIGURE 1. Flow chart for complete enumeration/exhaustive search method.

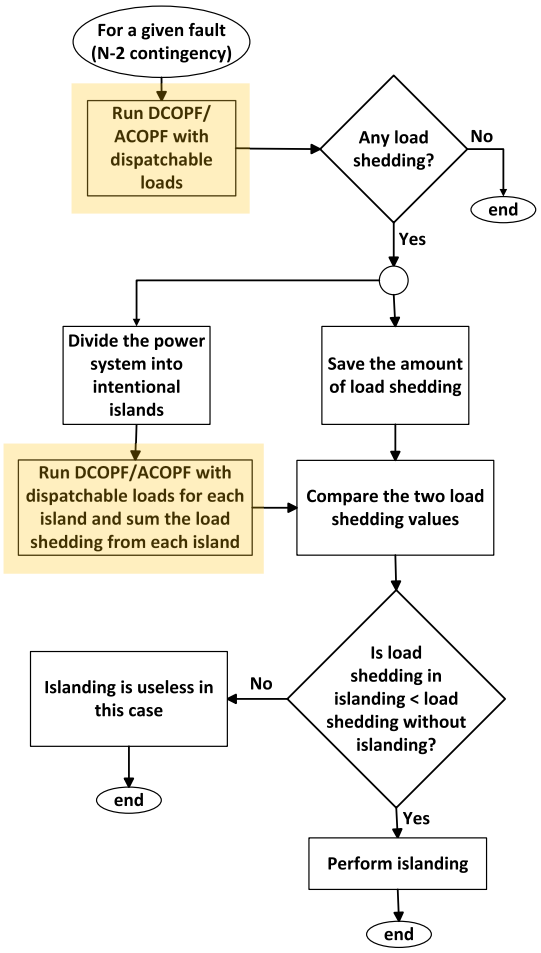

FIGURE 2. Flow chart for intentional islanding (IIS).

CE/ESM for the IEEE 118-bus system and achieves a LSR of 98%. As such, the performance of the LBTS and the LSB$_{max}$ algorithms, for the IEEE 118-bus system, indicate the need for another method with faster and accurate (i.e., higher LSR) operation. In this manuscript, we assume that maximum LSR is achieved by CE/ESM and refer to it as base case. The results of IIS are compared with the base case.

B. INTENTIONAL ISLANDING (IIS)

In order to avoid cascading failures, IIS is utilized to stabilize the system [7], [8], [28], [29]. IIS divides the power system into smaller independent subsystems, which are disconnected through a selected set of transmission lines known as ''cut set''. These islands are independent from each other and stable internally. It is important to keep the power frequency in the islanded region in an acceptable range and hence decrease the gap between generation and load.

The IIS algorithms proposed in [28] and [29] to mitigate cascading failures, focus on power system stability and are based on generator coherency. We propose to divide the power system into a pre-deterministic islands such that generation is greater than demand, i.e., $\sum_{i\in N_G} P^{G_i} > \sum_{j\in N_D} P^{D_j}$ in each island, as explained in Section IV-C. Moreover, in this work we develop four cases of creating islands to show that specific topologies may result in different amount of LSR. We leave the optimal method of creating islands for future work. The flow chart for IIS is shown in Fig. 2. For every non-trivial contingency, we divide the power system into predetermined islands as explained later in subsection IV-C. We then find the total load shedding by summing the load shedding in each island. The aim is to compare this total load shedding in IIS case with the load shedding achieved in TS case.

III. OPF FORMULATION FOR TS AND IIS

A. DCOPF FORMULATION

The electricity network is a set of N buses (or nodes) connected by a set of L transmission lines (or edges or branches), with controllable generators G and dispatchable demand D located at a subset $N_G \subseteq N$ and $N_D \subseteq N$ of the buses, respectively. The operating cost of a generator is a function of its active output power $c^i P^{G_i}$ where $i \in N_G$ [30]. The cost of load shedding is given by $c^j P^{D_j}$ where $j \in N_D$. The objective is to minimize the cost of generation and load shedding. DCOPF based formulation is given below:

$$min \quad \sum_{i\in N_G} c^i P^{G_i} + \sum_{j\in N_D} c^j P^{D_j} \tag{1}$$

$$\text{subject to} : \mathbf{B}.\theta = P^{G_i} - P^{D_j} \quad \forall\, i, j \in N \tag{2}$$

$$\sum_i P^{G_i} = \sum_i P^{D_i} \quad \forall\, i \in N \tag{3}$$

$$P^{G_i}_{min} \leq P^{G_i} \leq P^{G_i}_{max} \quad \forall\, i \in N_G \tag{4}$$
$$P^{D_j}_{min} \leq P^{D_j} \leq P^{D_j}_{max} \quad \forall\, j \in N_D \tag{5}$$
$$\left|\frac{1}{x^{ij}}(\theta^i - \theta^j)\right| \leq P^{ij}_{max} \quad \forall\, i,j \in N \tag{6}$$
$$\theta^i_{min} \leq \theta^i \leq \theta^i_{max} \quad \forall\, i \in N \tag{7}$$

All variables are either presented as matrices or vectors. P^{G_i} is the output of each generator and P^{D_j} is the power delivered at each load. P^{D_j} is dispatchable load and is modeled as "negative generation" with negative cost in the objective function. The interested reader is pointed to Section IV of [31] for details on the dispatchable loads. Since, P^{D_j} is negative, the value for c^j is negative to assign a positive cost for load shed, where c^j is a function of value of lost load (VoLL). Note that the cost associated with load shedding c^j in objective function (1) is larger than cost associated with generation c^i. Eq. (2) represents active power flow constraints. B is bus susceptance matrix and θ represents bus voltage angles. Power balance at each node is given by (3). Constraints (4)–(7) represent the generation limits for online generators, the load limits for dispatchable loads, the thermal limits on lines, and the minimum and maximum limits for the bus voltage angles, respectively.

B. ACOPF FORMULATION

For ACOPF-based formulation, the objective function (1) and constraints (4)–(7) remains unchanged. Additional constraints are given below:

$$S^{G_i} - S^{D_j} = diag(\overline{\mathbf{V}})\overline{\mathbf{Y}}^*_{bus}\overline{V}^* \quad \forall\, i,j \in N \tag{8}$$
$$\left|\overline{V}_i \overline{\mathbf{Y}}^{*\, i\to j}_{line,\ row-i}\overline{V}^*\right| \leq S^{i\to j}_{max} \quad \forall\, i,j \in N \tag{9}$$
$$\left|\overline{V}_j \overline{\mathbf{Y}}^{*\, j\to i}_{line,\ row-j}\overline{V}^*\right| \leq S^{j\to i}_{max} \quad \forall\, i,j \in N \tag{10}$$
$$\sum_i Q^{G_i} = \sum_j Q^{D_j} \quad \forall\, i,j \in N \tag{11}$$
$$Q^{G_i}_{min} \leq Q^{G_i} \leq Q^{G_i}_{max} \quad \forall\, i \in N_G \tag{12}$$
$$Q^{D_j}_{min} \leq Q^{D_j} \leq Q^{D_j}_{max} \quad \forall\, j \in N_D \tag{13}$$
$$V^i_{min} \leq V^i \leq V^i_{max} \quad \forall\, i \in N \tag{14}$$

Similar to DCOPF formulation, all variables are either matrices or vectors. Bar above a variable is used to present complex numbers. Complex conjugate is shown by operator $(.)^*$. Constraint (8) gives apparent power flow. $\overline{Y}_{bus}$ is the bus admittance matrix. Bidirectional apparent power flow line limits are presented by constraints (9) and (10). Constraints (11)–(13) are similar to (3)–(5) but for reactive power limits. Constraint (14) gives the maximum and minimum limits for the bus voltage magnitudes. Eq. (1)–(14) are adapted from [12].

IV. EXPERIMENTAL SETUP

A. COMPUTATIONAL ENVIRONMENT

Simulations are performed on a 3.89 GHz windows computer with 16 GB RAM without utilizing parallel processing. All simulations are performed using MATPOWER [31]. MATPOWER Interior Point Solver (MIPS) was used to run DCOPF with dispatchable loads [32].

TABLE 1. Details of the two test systems.

Test systems	# of buses	# of generators	# of branches
IEEE 39-bus	39	10	46
IEEE 118-bus	118	54	186

TABLE 2. Non-trivial CL for the two test systems.

Test systems	DCOPF L1 & L2 CL	ACOPF L1 & L2 CL
IEEE 39-bus	9	4
IEEE 118-bus	368	2770

B. TEST CASES

Two test cases are considered in this case study. Data from MATPOWER test cases is used for IEEE 39-bus system [33], [34]. Data from [35] is used for IEEE 118-bus system [36] with line limits taken from [37]. As in [11], our emergency ratings are set to 125% of normal ratings. Table 1 shows the details of the test systems used.

Authors in [38] removed the elements of the radial transmission system while using the IEEE 118-bus system in CL. This was done as the system would not be considered as N-1 compliant without the removal of the radial transmission elements in the N-1 CL and these elements are not subject to any standards of reliability as standardized by Federal Energy Regulatory Commission (FERC). Hence, we considered N-2 non-trivial line contingencies (L1 & L2) without including the radial transmission lines for the same reason mentioned in [38]. We developed a contingency list (CL) based on DCOPF and ACOPF formulation. CL is a list of contingencies that will overload the remaining components of power system. Non-trivial contingencies is a subset of CL that will result in nonzero load shed after a generation redispatch [11].

Note that we only considered N-2 non-trivial line contingencies (L1 & L2). N-2 contingencies that involve generator, i.e., G1 & L1 and G1 & G2, are beyond the scope of this work. The reason of not including generator contingencies in present work is that islands considered in this work are predetermined and a generator contingency might impact the rule on which islands are formed, i.e., $\sum_{i\in N_G} P^{G_i} > \sum_{j\in N_D} P^{D_j}$ in each island. Hence, forming optimal islands for contingencies involving generators is left for future work. Table 2 shows the non-trivial CL for the two test systems.

C. FORMATION OF AREAS AND ISLANDS

We divided IEEE 39-bus system and IEEE 118-bus system into three pre-determined areas as shown in Figs. 7 and 4. Note that division of these areas are not optimal but based on a rule mentioned in section II-B, i.e., $\sum_{i\in N_G} P^{G_i} > \sum_{j\in N_D} P^{D_j}$ in each area. For IEEE 39-bus system, we modified the areas

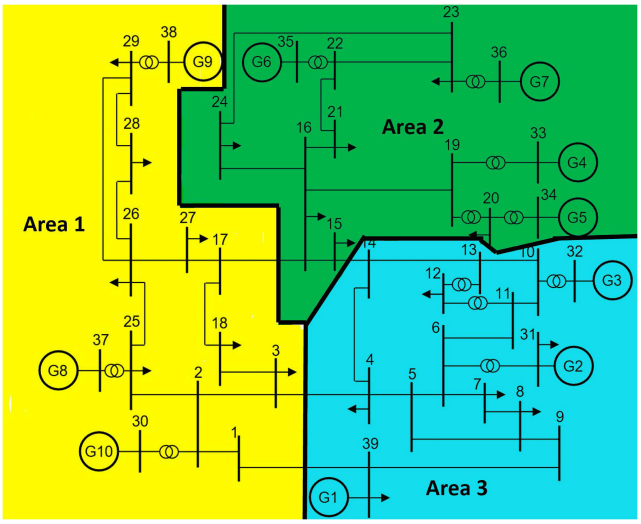

FIGURE 3. Division of IEEE 39-bus system into three areas.

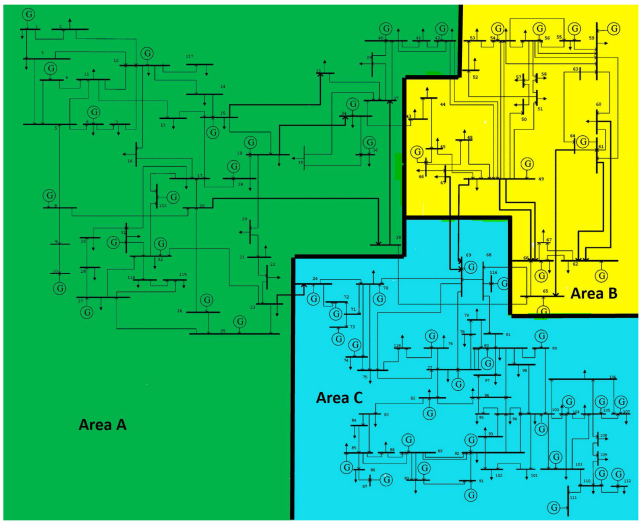

FIGURE 4. Division of IEEE 118-bus system into three areas.

defined in MATPOWER test case [33]. For IEEE 118-bus system, the areas are defined in [39]. The interested reader is pointed to [33] and [39], for more details on mathematical formulation of cutsets and areas. The cut set used for IEEE 39-bus system is between buses 14-15, 4-3, 39-1, 16-17 and is shown in Table 3. Similarly, the cut set used for IEEE 118-bus system is between buses 23-24, 38-65,47-69, 49-69, 65-68, 37-43, 42-49 and is shown in Table 4.

1) IIS FOR IEEE 39-BUS SYSTEM

Table 3 shows the four cases of islanding created by mixing different area combinations for IEEE 39-bus system. "Islanding 4" is created by dividing IEEE 39-bus system into three islands where each island is equal to an area. Note that all three areas have $\sum_{i\in N_G} P^{G_i} > \sum_{j\in N_D} P^{D_j}$. "Islanding 1" is created by dividing the system in two islands, i.e., combining area 1 and area 2 as one island while area 3 is considered a separate island. Similarly, "islanding 2" and "islanding 3" have two islands in each case as shown in Table 3. Transmission line cut set in Table 3 shows which transmission lines are required to cut to obtain the four cases of islanding. The idea here is to show that different way of islanding a power system may result in different LSR.

2) IIS FOR IEEE 118-BUS SYSTEM

Table 4 shows the four cases of islanding created by mixing different area combinations for IEEE 118-bus system. To differentiate islanding names from IEEE 39-bus system, we used letters instead of numbers for IEEE 118-bus system. "Islanding D" is created by dividing IEEE 118-bus system into three islands where each island is equal to an area. Note that all three areas have $\sum_{i\in N_G} P^{G_i} > \sum_{j\in N_D} P^{D_j}$. "Islanding A" is created by dividing the system in two islands, i.e., combining area A and area B as one island while area C is considered a separate island. Similarly, "islanding B" and "islanding C" have two islands in each case as shown in Table 4. Transmission line cut set in Table 4 shows which transmission lines are required to cut to obtain the four cases of islanding.

D. METRICS

As mentioned above, if there exists the best TS candidate, the base case (i.e., CE/ESM) will find it. Hence, we assume that the maximum LSR (i.e., 100%) is achieved by the base case and we will compare the IIS algorithm with the base case. Three solution metrics from [12], namely the percentage load shed reduction (%LSR), the worst speedup (WS), and the average speedup are used to compare LSR and computational efficiency of the IIS algorithm with base case.

The idea is to see if IIS algorithm performs faster than the CE/ESM, but should be capable of achieving the %LSR of the CE/ESM. LSR in the CE/ESM and the IIS is given by (15), where τ is ESM or IIS and (LS_i) is load shed during contingency i where, $i \in \{CL\}$.

$$\text{LSR}_\tau = \sum_{i=1}^{CL} (LS_i)_{without\ \tau} - \sum_{i=1}^{CL} (LS_i)_\tau \tag{15}$$

%LSR for IIS is given by (16).

$$\%\text{LSR} = \frac{\text{LSR}_{IIS}}{\text{LSR}_{CE/ESM}} \times 100 \tag{16}$$

To compare the computational performance of the IIS algorithm with the CE/ESM, we assume that the CE/ESM has a speed (unit-less quantity) of one. IIS algorithm with speed of greater than one means that the IIS algorithm is faster than the CE/ESM. Moreover, from the entire CL, we want to compare the maximum time taken by IIS algorithm, i.e., the worst case with the worst case in CE/ESM. Speedup in the worst case is given by (17).

$$\text{WS} = \frac{T_{max.\ CE/ESM}}{T_{max.\ IIS}} \geq 1 \tag{17}$$

TABLE 3. Intentional Islanding (IIS) for IEEE 39-bus system.

	Areas	P_G (MW)	P_D (MW)	Transmission line cut set between buses
Islanding 1	Area 1 + Area 2	4940	4095	14-15, 4-3, 39-1
	Area 3	2427	2159	
Islanding 2	Area 1 + Area 3	4898	4543	14-15, 16-17
	Area 2	2469	1711	
Islanding 3	Area 2 + Area 3	4896	3870	16-17, 39-1, 3-4
	Area 1	2471	2384	
Islanding 4	Area 1	2471	2384	16-17, 14-15, 3-4, 1-39
	Area 2	2469	1711	
	Area 3	2427	2159	

TABLE 4. Intentional Islanding (IIS) for IEEE 118-bus system.

	Areas	P_G (MW)	P_D (MW)	Transmission line cut set between buses
Islanding A	Area A + Area B	4940	4095	23-24, 38-65, 47-69, 49-69, 68-65
	Area C	2427	2159	
Islanding B	Area A + Area C	4898	4543	43-34, 42-49, 47-69, 49-69, 65-68
	Area B	2469	1711	
Islanding C	Area B + Area C	4896	3870	23-24, 34-43, 42-49, 38-65
	Area A	2471	2384	
Islanding D	Area A	2471	2384	23-24, 38-65,47-69, 49-69, 65-68, 34-43, 42-49
	Area B	2469	1711	
	Area C	2427	2159	

The average speedup (S_μ) achieved by the IIS algorithm is the ratio of average time taken by the IIS algorithm ($T_{\mu\ IIS}$) for the CL to the average time taken by the CE/ESM algorithm ($T_{\mu\ CE/ESM}$). S_μ is given by (18).

$$\mathrm{S}_\mu = \frac{T_{\mu\ CE/ESM}}{T_{\mu\ IIS}} \geq \mathrm{WS} \tag{18}$$

V. SIMULATION RESULTS

A. DCOPF FORMULATION BASED SIMULATION RESULTS

Fig. 5 shows the comparison between DCOPF formulation based base case (CE/ESM) and DCOPF formulation based IIS for IEEE 39-bus system. Note that %LSR of base case (CE/ESM) is 100%. Moreover, WS of base case is taken as one. For IEEE 39-bus system, total load shedding for CL without using TS or IIS algorithms is 1884 *MW*. Amount of load shedding after TS is 1494 *MW*. The amount of load shedding after islanding 3 is 689 *MW*. %LSR in islanding 3 is three times more than base case. These results show that IIS can perform better than TS. Moreover, the WS of islanding 3 is 23 times faster than base case. The reason for this speedup is that in IIS algorithm we divided the system into small islands as shown in flow chart of Fig. 2. Running DCOPF for small islands is faster than CE/ESM.

Fig. 6 shows the comparison between DCOPF formulation based base case (CE/ESM) and DCOPF formulation based IIS for IEEE 118-bus system. Note that, for %LSR, islanding A, B, C, and D performed better than TS base case. Islanding A %LSR is 120% of base case with speedup of 87 times of the base case. From Figs. 5 and 6, we can conclude that DCOPF formulation based IIS has potential for better LSR and improved computational performance as compared to DCOPF formulation based TS.

B. ACOPF FORMULATION BASED SIMULATION RESULTS

Fig. 7 shows the comparison between ACOPF formulation based base case (CE/ESM) and ACOPF formulation based

FIGURE 5. Comparison of DCOPF formulation based base case (CE/ESM) and DCOPF formulation based IIS for IEEE 39-bus system.

FIGURE 6. Comparison of DCOPF formulation based base case (CE/ESM) and DCOPF formulation based IIS for IEEE 118-bus system.

IIS for IEEE 39-bus system. Note that %LSR of base case (CE/ESM) is 100%. Moreover, WS of base case is taken as one. Note that none of the IIS cases performed better than the TS base case but IIS performed computationally fast than the base case. %LSR achieved by islanding 2 is 74% of the base case with the speedup of 10.6 times compared to base case.

Figs. 8 shows the comparison between ACOPF formulation based base case (CE/ESM) and ACOPF formulation

FIGURE 7. Comparison of ACOPF formulation based base case (CE/ESM) and ACOPF formulation based IIS for IEEE 39-bus system.

FIGURE 8. Comparison of ACOPF formulation based base case (CE/ESM) and ACOPF formulation based IIS for IEEE 118-bus system.

based IIS for IEEE 118-bus system. Note that, for %LSR, islanding A, B, C, and D performed better than TS base case. Islanding A %LSR is 205% of base case with speedup of 89 times of the base case. From Figs. 7 and 8, we can conclude that ACOPF formulation based IIS has potential for better LSR and improved computational performance as compared to ACOPF formulation based TS.

C. AVERAGE SPEEDUP VS. WORST SPEEDUP

Figs. 5-8 show that the WS improved from the smaller (i.e., the IEEE 39-bus system) to the larger test system (i.e., the IEEE 118-bus system). The reason is that the number of transmission lines increases for larger test system, which makes the base case computationally expensive. On the other hand, IIS algorithm divides the system into small islands which reduces the computational burden hence WS increases as we move from smaller test case to larger test cases. This feature of scalability helps to implement IIS to real world larger systems. Moreover, Figs. 9 - 12 show that the average speedup gained by IIS is larger than the WS, which means most of the contingencies in CL take lesser time than the time taken by the worst contingency.

D. COMPARISONS OF IIS WITH LBTS AND LSB_{max} ALGORITHMS

Results presented in section V showed that IIS has potential to perform better than TS base case in terms of LSR. The aim of this section is to compare the computational performance of

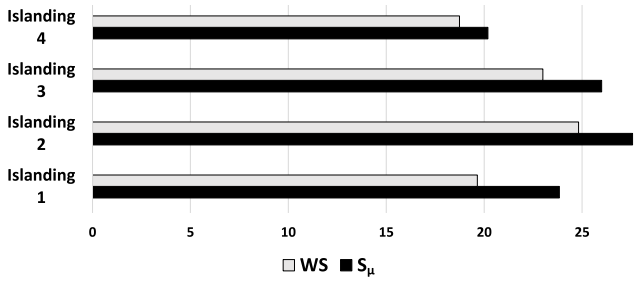

FIGURE 9. Comparison of DCOPF formulation based average speedup vs. worst speedup for IEEE 39-bus system.

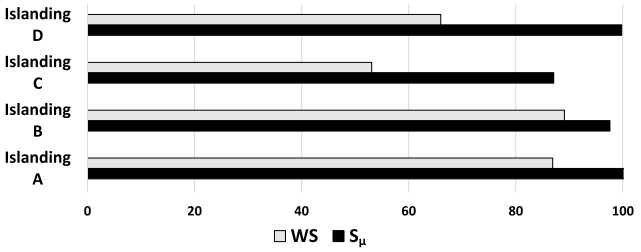

FIGURE 10. Comparison of DCOPF formulation based average speedup vs. worst speedup for IEEE 118-bus system.

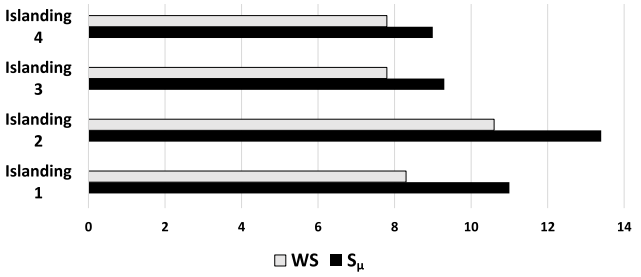

FIGURE 11. Comparison of ACOPF formulation based average speedup vs. worst speedup for IEEE 39-bus system.

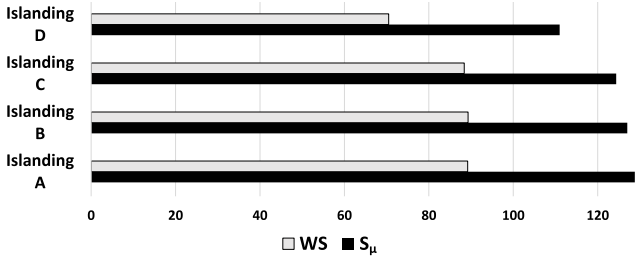

FIGURE 12. Comparison of ACOPF formulation based average speedup vs. worst speedup for IEEE 118-bus system.

the IIS algorithm with two existing computationally fast TS algorithms, other than CE/ESM, from literature. LBTS [13] and LSB_{max} [12] showed computational superiority compared to CE/ESM.

1) DCOPF FORMULATION BASED COMPARISON

Table 5 compares the performance of the DCOPF formulation based IIS algorithm with the DCOPF formulation

TABLE 5. Comparison of the performance of the DCOPF formulation based IIS algorithm with DCOPF formulation based LBTS and LSB$_{max}$ algorithms for the IEEE 39 and IEEE 118-bus test systems. For IIS algorithm, we selected islanding 3 and islanding B for the IEEE 39 and IEEE 118-bus test systems, respectively.

		IEEE 39-bus	IEEE 118-bus
LBTS	%LSR	-	5.2
	S_μ	-	108
LSB$_{max}$	%LSR	100	99
	S_μ	4.6	22
Intentional Islanding	%LSR	306	120
	S_μ	26	112.8

TABLE 6. Comparison of the performance of the ACOPF formulation based IIS algorithm with ACOPF formulation based LBTS and LSB$_{max}$ algorithms for the IEEE 39 and IEEE 118-bus test systems. For IIS algorithm, we selected islanding 2 and islanding A for the IEEE 39 and IEEE 118-bus test systems, respectively.

		IEEE 39-bus	IEEE 118-bus
LBTS	%LSR	-	15.4
	S_μ	-	70.7
LSB$_{max}$	%LSR	85	85
	S_μ	4.6	11.4
Intentional Islanding	%LSR	74.3	205
	S_μ	13.4	128.8

based LBTS and LSB$_{max}$ algorithms. Note that the %LSR and S_μ for each algorithm are calculated with respect to the innate CE/ESM, i.e., using (16) and (18), respectively. By transitivity, we can establish the comparison of the IIS algorithm with LSB$_{max}$ and LBTS algorithms through their respective CE/ESM. For both test cases, i.e., IEEE 39-bus and IEEE 118-bus test system, the IIS algorithm not only achieves a higher %LSR, but is faster than LBTS and LSB$_{max}$ algorithms.

2) ACOPF FORMULATION BASED COMPARISON

Table 6 compares the performance of the ACOPF formulation based IIS algorithm with the ACOPF formulation based LBTS and LSB$_{max}$ algorithms. Note that the %LSR and S_μ for each algorithm are calculated with respect to the innate CE/ESM, i.e., using (16) and (18), respectively. Again, by transitivity, we can establish the comparison of the IIS algorithm with LSB$_{max}$ and LBTS algorithms through their respective CE/ESM. For both test cases, i.e., IEEE 39-bus and IEEE 118-bus test system, the IIS algorithm achieves a higher computational performance compared to LBTS and LSB$_{max}$ algorithms. For IEEE 118-bus test system, the %LSR achieved by the IIS algorithm is greater than the %LSR achieved by LBTS and LSB$_{max}$ algorithms.

E. COMPARISON OF ISLANDING A WITH ISLANDING B, C, AND D FOR IEEE 118-BUS SYSTEM

Results above showed that different islanding topology yields different LSR. The aim of this section is to show that one islanding topology is not optimal for every contingency. Similar to finding best TS candidate, there is a need to find optimal islanding for each contingency, and is left for future work.

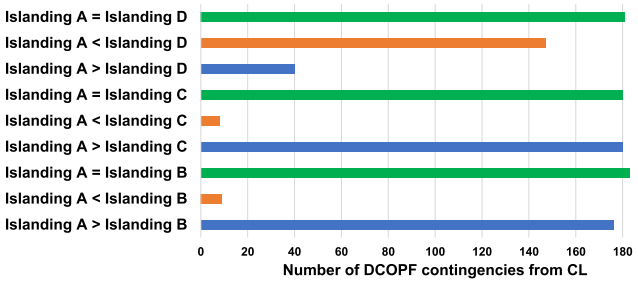

FIGURE 13. DCOPF based comparison of islanding A with islandings B, C, and D for IEEE 118-bus system.

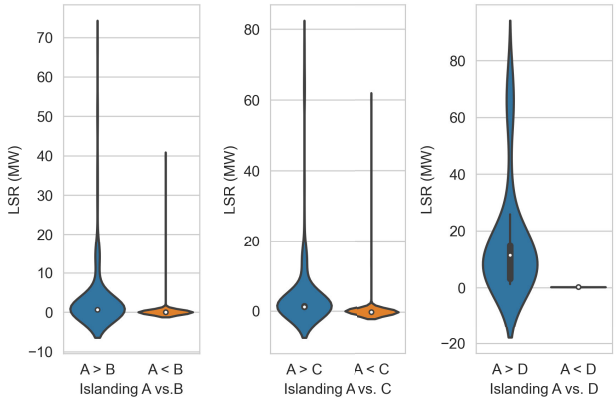

FIGURE 14. DCOPF based violin plot for the distribution of the difference of LSR achieved (in MW) for the cases where islanding A performs better or worst than islanding B, C, and D, respectively.

1) DCOPF FORMULATION BASED COMPARISON

Fig. 6 shows that, for DCOPF formulation based %LSR, islanding A performed better than islandings B, C, and D. Fig. 13 presents the contingency by contingency comparison of islanding A with islandings B, C, and D. Out of 368 total N-2 non-trivial L1 & L2 contingency cases, islanding A recovered less load shedding than islanding D in 147 cases. These results showed that islanding A is not the optimal islanding topology for 147 cases. On the other hand, out of 368 total N-2 non-trivial L1 & L2 contingency cases, islanding A recovered higher load shedding than islanding D in 40 cases. But, the difference in LSR between islanding A vs. islanding D for these 40 cases is higher than compared to 147 cases. That is the reason why the overall result for islanding A is better than islanding D. Fig. 14 shows the violin plot for the distribution of the difference of LSR achieved (in MW) for the cases where islanding A performs better or worst than islanding B, C, and D, respectively.

2) ACOPF FORMULATION BASED COMPARISON

Fig. 8 showed that, for ACOPF formulation based %LSR, islanding A performed better than islandings B, C, and D. Fig. 15 presents the contingency by contingency comparison of islanding A with islandings B, C, and D. Out of 2770 total N-2 non-trivial L1 & L2 contingency cases, islanding A

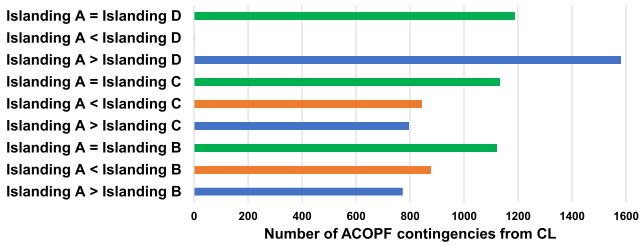

FIGURE 15. ACOPF based comparison of islanding A with islandings B, C, and D for IEEE 118-bus system.

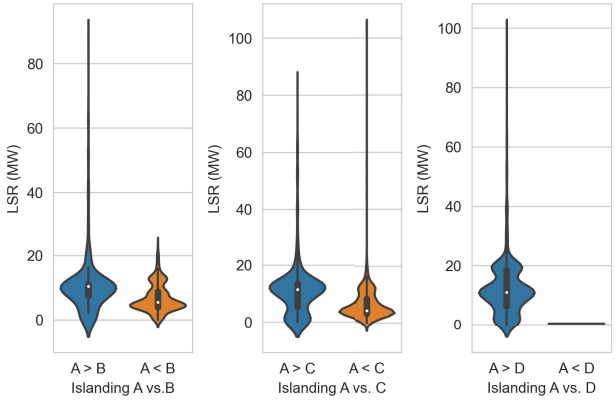

FIGURE 16. ACOPF based violin plot for the distribution of the difference of LSR achieved (in MW) for the cases where islanding A performs better or worst than islanding B, C, and D, respectively.

recovered less load shedding than islanding B in 876 cases. These results showed that islanding A is not the optimal islanding topology for 876 cases. On the other hand, out of 2770 total N-2 non-trivial L1 & L2 contingency cases, islanding A recovered higher load shedding than islanding B in 773 cases. But, the difference in LSR between islanding A vs. islanding D for these 773 cases is higher than compared to 876 cases. That is the reason why the overall result for islanding A is better than islanding B. Fig. 16 shows the violin plot for the distribution of the difference of LSR achieved (in MW) for the cases where islanding A performs better or worst than islanding B, C, and D, respectively.

VI. CONCLUSION

Load shedding is the least priority of power system operators but under emergency conditions, operators are forced to perform load shedding to maintain the power system stability and security. Topology control can reduce the required amount of load shedding after a contingency. In this paper, we explored intentional islanding as a load shed recovery (LSR) mechanism. We compared the load shed recovery mechanism based on intentional islanding with complete enumeration or exhaustive search method. We implemented the algorithm on IEEE 39-bus system and IEEE 118-bus system for N-2 non-trivial L1 & L2 contingencies. The %LSR achieved by the DCOPF formulation based intentional islanding for IEEE 39-bus system is three times higher than the the DCOPF formulation based complete enumeration or exhaustive search algorithm. The %LSR achieved by the DCOPF formulation based intentional islanding for IEEE 118-bus system is 1.2 times higher than the the DCOPF formulation based complete enumeration or exhaustive search algorithm. Similarly, the %LSR achieved by the ACOPF formulation based intentional islanding for IEEE 118-bus system is two times higher than the the ACOPF formulation based complete enumeration or exhaustive search algorithm. These results show that intentional islanding can be a potential solution for load shed recovery with notable speedup. The speedup of intentional islanding algorithm increases as we move from smaller system to larger system which is a good indication that intentional islanding based load shed recovery algorithm is scalable. Comparison of the intentional islanding algorithm with existing TS algorithms showed the computational superiority of the intentional islanding algorithm. In future, we will use parallel programming to further increase the achieved speedup.

ACKNOWLEDGMENT

The authors would like to thank Dr. Robert Fourney from South Dakota State University for discussions on intentional islanding during the course EE-692.

REFERENCES

[1] A. Nordrum. *Transmission Failure Causes Nationwide Blackout in Argentina*. Accessed: May 15, 2020. [Online]. Available: https://tinyurl.com/y8jk6l7f

[2] M. Sinha, M. Panwar, R. Kadavil, T. Hussain, S. Suryanarayanan, and M. Papic, "Optimal load shedding for mitigation of cascading failures in power grids," in *Proc. 10th ACM Int. Conf. Future Energy Syst.*, Jun. 2019, pp. 416–418.

[3] X. Li and K. W. Hedman, "Enhanced energy management system with corrective transmission switching strategy: Methodology—Part I," *IEEE Trans. Power Syst.*, vol. 34, no. 6, pp. 4490–4502, Nov. 2019.

[4] X. Li and K. W. Hedman, "Enhanced energy management system with corrective transmission switching strategy—Part II: Results and discussion," *IEEE Trans. Power Syst.*, vol. 34, no. 6, pp. 4503–4513, Nov. 2019.

[5] S. Fattahi, J. Lavaei, and A. Atamturk, "A bound strengthening method for optimal transmission switching in power systems," *IEEE Trans. Power Syst.*, vol. 34, no. 1, pp. 280–291, Jan. 2019.

[6] M. Sheikh, J. Aghaei, A. Letafat, M. Rajabdorri, T. Niknam, M. Shafie-Khah, and J. P. Catalão, "Security-constrained unit commitment problem with transmission switching reliability and dynamic thermal line rating," *IEEE Syst. J.*, vol. 13, no. 4, pp. 3933–3943, Dec. 2019.

[7] Z. Liu, A. Clark, L. Bushnell, D. S. Kirschen, and R. Poovendran, "Controlled islanding via weak submodularity," *IEEE Trans. Power Syst.*, vol. 34, no. 3, pp. 1858–1868, May 2019.

[8] W. Ju, K. Sun, and R. Yao, "Interaction graph-based active islanding to mitigate cascading outages," in *Proc. IEEE Power Energy Soc. Gen. Meeting (PESGM)*, Aug. 2019, pp. 1–5.

[9] X. Li, P. Balasubramanian, M. Sahraei-Ardakani, M. Abdi-Khorsand, K. W. Hedman, and R. Podmore, "Real-time contingency analysis with corrective transmission switching," *IEEE Trans. Power Syst.*, vol. 32, no. 4, pp. 2604–2617, Jul. 2017.

[10] W. E. Brown and E. Moreno-Centeno, "Transmission-line switching for load shed prevention via an accelerated linear programming approximation of AC power flows," *IEEE Trans. Power Syst.*, vol. 35, no. 4, pp. 2575–2585, Jul. 2020.

[11] A. R. Escobedo, E. Moreno-Centeno, and K. W. Hedman, "Topology control for load shed recovery," *IEEE Trans. Power Syst.*, vol. 29, no. 2, pp. 908–916, Mar. 2014.

[12] T. Hussain, S. M. S. Alam, T. M. Hansen, and S. Suryanarayanan, "The LSB_{max} algorithm for boosting resilience of electric grids post (N-2) contingencies," *J. Eng.*, vol. 2021, no. 12, pp. 807–816, Dec. 2021. [Online]. Available: https://ietresearch.onlinelibrary.wiley.com/doi/abs/10.1049/tje2.12081
[13] T. Hussain, S. Suryanarayanan, T. M. Hansen, and S. M. S. Alam, "A computationally improved heuristic algorithm for transmission switching using line flow thresholds for load shed reduction," in *Proc. IEEE Madrid PowerTech*, Jul. 2021, pp. 1–6.
[14] J. D. Lyon, S. Maslennikov, M. Sahraei-Ardakani, T. Zheng, E. Litvinov, X. Li, P. Balasubramanian, and K. W. Hedman, "Harnessing flexible transmission: Corrective transmission switching for ISO-NE," *IEEE Power Energy Technol. Syst. J.*, vol. 3, no. 3, pp. 109–118, Sep. 2016.
[15] M. Khanabadi, H. Ghasemi, and M. Doostizadeh, "Optimal transmission switching considering voltage security and N-1 contingency analysis," *IEEE Trans. Power Syst.*, vol. 28, no. 1, pp. 542–550, Feb. 2013.
[16] M. Abdi-Khorsand, M. Sahraei-Ardakani, and Y. Al-Abdullah, "Corrective transmission switching for N-1-1 contingency analysis," in *Proc. IEEE Power Energy Soc. Gen. Meeting*, Jul. 2017, p. 1.
[17] X. Liu, Y. Wen, and Z. Li, "Multiple solutions of transmission line switching in power systems," *IEEE Trans. Power Syst.*, vol. 33, no. 1, pp. 1118–1120, Jan. 2018.
[18] Y. Sang and M. Sahraei-Ardakani, "The interdependence between transmission switching and variable-impedance series FACTS devices," *IEEE Trans. Power Syst.*, vol. 33, no. 3, pp. 2792–2803, May 2018.
[19] Z. Yang and S. Oren, "Line selection and algorithm selection for transmission switching by machine learning methods," in *Proc. IEEE Milan PowerTech*, Jun. 2019, pp. 1–6.
[20] J. Bélanger, L. A. Dessaint, and I. Kamwa, "An extended optimal transmission switching algorithm adapted for large networks and hydro-electric context," *IEEE Access*, vol. 8, pp. 87762–87774, 2020.
[21] K. Garifi, E. S. Johnson, B. Arguello, and B. J. Pierre, "Transmission grid resiliency investment optimization model with SOCP recovery planning," *IEEE Trans. Power Syst.*, vol. 37, no. 1, pp. 26–37, Jan. 2022.
[22] S. M. Mohseni-Bonab, I. Kamwa, A. Rabiee, and C. Y. Chung, "Stochastic optimal transmission switching: A novel approach to enhance power grid security margins through vulnerability mitigation under renewables uncertainties," *Appl. Energy*, vol. 305, Jan. 2022, Art. no. 117851.
[23] M. Meneses, E. Nascimento, L. H. Macedo, and R. Romero, "Transmission network expansion planning considering line switching," *IEEE Access*, vol. 8, pp. 115148–115158, 2020.
[24] T. Hussain, S. Suryanarayanan, T. M. Hansen, and S. M. S. Alam, "A fast and scalable transmission switching algorithm for boosting resilience of electric grids impacted by extreme weather events," *IEEE Access*, vol. 10, pp. 57893–57901, 2022.
[25] T. Hussain, S. Suryanarayanan, and S. S. M. Alam, "Hybridized transmission switching for contingency management in electric power systems," International Application Patent 21 26 540, Apr. 9, 2021.
[26] M. Sahraei-Ardakani, X. Li, P. Balasubramanian, K. W. Hedman, and M. Abdi-Khorsand, "Real-time contingency analysis with transmission switching on real power system data," *IEEE Trans. Power Syst.*, vol. 31, no. 3, pp. 2501–2502, May 2016.
[27] C. Coffrin and P. Van Hentenryck, "A linear-programming approximation of AC power flows," *INFORMS J. Comput.*, vol. 26, no. 4, pp. 718–734, Nov. 2014.
[28] A. Esmaeilian and M. Kezunovic, "Prevention of power grid blackouts using intentional islanding scheme," *IEEE Trans. Ind. Appl.*, vol. 53, no. 1, pp. 622–629, Jan. 2017.
[29] M. Dabbaghjamanesh, B. Wang, A. Kavousi-Fard, S. Mehraeen, N. D. Hatziargyriou, D. N. Trakas, and F. Ferdowsi, "A novel two-stage multi-layer constrained spectral clustering strategy for intentional islanding of power grids," *IEEE Trans. Power Del.*, vol. 35, no. 2, pp. 560–570, Apr. 2020.
[30] M. F. Zia, E. Elbouchikhi, and M. E. H. Benbouzid, "An energy management system for hybrid energy sources-based stand-alone marine microgrid," *IOP Conf. Ser., Earth Environ. Sci.*, vol. 322, no. 1, Aug. 2019, Art. no. 012001.
[31] R. D. Zimmerman, C. E. Murillo-Sánchez, and R. J. Thomas, "MATPOWER: Steady-state operations, planning, and analysis tools for power systems research and education," *IEEE Trans. Power Syst.*, vol. 26, no. 1, pp. 12–19, Feb. 2011.
[32] H. Wang, C. E. Murillo-Sanchez, R. D. Zimmerman, and R. J. Thomas, "On computational issues of market-based optimal power flow," *IEEE Trans. Power Syst.*, vol. 22, no. 3, pp. 1185–1193, Aug. 2007.
[33] M. Pai, *Energy Function Analysis for Power System Stability*. New York, NY, USA: Springer, 2012.
[34] Matpower. *Case39*. Accessed: Sep. 5, 2021. [Online]. Available: https://tinyurl.com/925xstf3
[35] R. Christie, "Power systems test case archive," Dept. Elect. Eng., Univ. Washington, Apr. 2000. [Online]. Available: http://www.ee.washington.edu/research/pstca
[36] Matpower. *Case118*. Accessed: Sep. 5, 2021. [Online]. Available: https://tinyurl.com/sr93fc7a
[37] S. Blumsack, *Network Topologies and Transmission Investment Under Electric-Industry Restructuring*. Pittsburgh, PA, USA: Carnegie Mellon Univ., 2006.
[38] K. W. Hedman, R. P. O'Neill, E. B. Fisher, and S. S. Oren, "Optimal transmission switching with contingency analysis," *IEEE Trans. Power Syst.*, vol. 24, no. 3, pp. 1577–1586, Aug. 2009.
[39] H. M. Dola and B. H. Chowdhury, "Intentional islanding and adaptive load shedding to avoid cascading outages," in *Proc. IEEE Power Eng. Soc. Gen. Meeting*, Jun. 2006, p. 8.

TANVEER HUSSAIN (Member, IEEE) received the B.E. degree in electrical engineering from the National University of Sciences and Technology, Islamabad, Pakistan, the M.S. degree in electrical engineering from the Politecnico di Milano, Milan, Italy, and the Ph.D. degree in electrical engineering from South Dakota State University, Brookings, South Dakota. He is currently a Postdoctoral Research Associate with the Idaho National Laboratory, Idaho Falls, Idaho. His research interests include the topic of wide-area transmission systems and minimization of load shedding.

SAIMA ISHAQ (Graduate Student Member, IEEE) received the B.E. and M.S. degrees in electrical engineering with a major in power systems. She is currently pursuing the Graduate degree with the Electrical Engineering and Computer Science Department, South Dakota State University, USA. Her research interests include data-driven modeling, simulation, and optimization of renewable energy systems.

SHEROZE LIAQAT received the bachelor's and master's degrees in electrical engineering with specialization in power systems from the University of Engineering and Technology Lahore, Lahore, in 2018 and 2020, respectively. He is currently pursuing the Ph.D. degree with the Electrical Engineering and Computer Science Department, South Dakota State University, USA. He served as the Faculty Member with the Electrical Engineering Department, National University of Computer and Emerging Sciences, Lahore, Pakistan, from 2018 to 2021. His current research interests include the application of meta-heuristic techniques, soft computing methods, machine learning algorithms in the economic dispatch problem, and electricity markets.

MUHAMMAD FAHAD ZIA (Member, IEEE) received the Ph.D. degree in electrical engineering from the University of Brest, Brest, France, in 2020. His research interests and experience include AC/DC microgrids, energy management systems, power system operation, cyber-physical systems security, and power electronics. He is serving as a Reviewer for many prestigious journals from IEEE, IET, Elsevier, MPDI, and other publishers, including IEEE TRANSACTIONS ON SMART GRID, IEEE TRANSACTIONS ON SYSTEMS, MAN, AND CYBERNETICS: SYSTEMS, IEEE TRANSACTIONS ON INDUSTRY APPLICATION, *IET Renewable Power Generation*, *IET Generation, Transmission & Distribution*, *Electric Power Systems Research*, and *Energies* among others.

AHMED AL-DURRA (Senior Member, IEEE) received the Ph.D. degree in ECE from The Ohio State University, in 2010. He is currently a Professor with the EECS Department, Khalifa University, United Arab Emirates. He has one U.S. patent, one edited book, 12 book chapters, and over 230 scientific papers in top-tier journals and refereed international conference proceedings. He has supervised/co-supervised over 30 Ph.D./master's students. He is leading the Energy Systems Control and Optimization Laboratory under the Advanced Power and Energy Center. His research interests include applications of control and estimation theory on power systems stability, micro and smart grids, renewable energy systems and integration, and process control. He is an Editor of IEEE TRANSACTIONS ON SUSTAINABLE ENERGY and IEEE POWER ENGINEERING LETTERS and an Associate Editor of IEEE TRANSACTIONS ON INDUSTRY APPLICATIONS, *IET Renewable Power Generation*, and *Frontiers in Energy Research*.

BASEEM KHAN (Senior Member, IEEE) received the B.Eng. degree in electrical engineering from Rajiv Gandhi Technological University, Bhopal, India, in 2008, and the M.Tech. and D.Phil. degrees in electrical engineering from the Maulana Azad National Institute of Technology, Bhopal, in 2010 and 2014, respectively. He is currently working as a Faculty Member at Hawassa University, Ethiopia. His research interests include power system restructuring, power system planning, smart grid technologies, meta-heuristic optimization techniques, reliability analysis of renewable energy systems, power quality analysis, and renewable energy integration. He has published more than 100 research articles in well reputable research journals, including IEEE TRANSACTION, IEEE ACCESS, *Computer and Electrical Engineering* (Elsevier), *IET GTD*, *IET PRG*, and *IET Power Electronics*. Further, he has published authored and edited books with Wiley, CRC Press, and Elsevier.

JOSEP M. GUERRERO (Fellow, IEEE) received the B.S. degree in telecommunications engineering, the M.S. degree in electronics engineering, and the Ph.D. degree in power electronics from the Technical University of Catalonia, Barcelona, in 1997, 2000, and 2003, respectively. Since 2011, he has been a Full Professor with the Department of Energy Technology, Aalborg University, Denmark, where he is responsible for the Microgrid Research Program. Since 2014, he has been a Chair Professor with Shandong University. Since 2015, he has been a Distinguished Guest Professor with Hunan University, and since 2016, he has been a Visiting Professor Fellow at Aston University, U.K., and a Guest Professor at the Nanjing University of Posts and Telecommunications. In 2019, he became a Villum Investigator by The Villum Fonden, which supports the Center for Research on Microgrids (CROM), Aalborg University, where being the Founder and the Director (www.crom.et.aau.dk). His research interests include different microgrid aspects, including power electronics, distributed energy-storage systems, hierarchical and cooperative control, energy management systems, smart metering, the Internet of Things for AC/DC microgrid clusters, and islanded minigrids. Specially focused on microgrid technologies applied to offshore wind, maritime microgrids for electrical ships, vessels, ferries and seaports, and space microgrids applied to nanosatellites and spacecrafts. He has published more than 600 journal articles in the fields of microgrids and renewable energy systems, which are cited more than 50,000 times. He received the Best Paper Award of the IEEE TRANSACTIONS ON ENERGY CONVERSION, from 2014 to 2015, and the Best Paper Prize of IEEE-PES, in 2015. As well, he received the Best Paper Award of the *Journal of Power Electronics*, in 2016. During six consecutive years, from 2014 to 2019, he was awarded by Clarivate Analytics (former Thomson Reuters) as a Highly Cited Researcher with 50 highly cited papers. In 2015, he was elevated as IEEE Fellow for his contributions on ''distributed power systems and microgrids.''